NANO LETTERS

Letter

pubs.acs.org/NanoLett

P-Type Polymer-Hybridized High-Performance Piezoelectric Nanogenerators

Keun Young Lee,[†] Brijesh Kumar,[†] Ju-Seok Seo,[†] Kwon-Ho Kim,[†] Jung Inn Sohn,[‡] Seung Nam Cha,[‡] Dukhyun Choi,*[,§] Zhong Lin Wang,*[,∥] and Sang-Woo Kim*[,†,⊥]

[†]School of Advanced Materials Science and Engineering and [⊥]SKKU Advanced Institute of Nanotechnology (SAINT), Center for Human Interface Nanotechnology (HINT), Sungkyunkwan University (SKKU), Suwon 440-746, Republic of Korea

[‡]Samsung Advanced Institute of Technology, Yongin, Gyeonggi, 446−712, Republic of Korea

[§]Department of Mechanical Engineering, Kyung Hee University, Yongin 446-701, Republic of Korea

[∥]School of Materials Science and Engineering, Georgia Institute of Technology, Atlanta, Georgia 30332-0245, United States

S *Supporting Information*

ABSTRACT: Enhancing the output power of a nanogenerator is essential in applications as a sustainable power source for wireless sensors and microelectronics. We report here a novel approach that greatly enhances piezoelectric power generation by introducing a p-type polymer layer on a piezoelectric semiconducting thin film. Holes at the film surface greatly reduce the piezoelectric potential screening effect caused by free electrons in a piezoelectric semiconducting material. Furthermore, additional carriers from a conducting polymer and a shift in the Fermi level help in increasing the power output. Poly(3-hexylthiophene) (P3HT) was used as a p-type polymer on piezoelectric semiconducting zinc oxide (ZnO) thin film, and phenyl-C_{61}-butyric acid methyl ester (PCBM) was added to P3HT to improve carrier transport. The ZnO/P3HT:PCBM-assembled piezoelectric power generator demonstrated 18-fold enhancement in the output voltage and tripled the current, relative to a power generator with ZnO only at a strain of 0.068%. The overall output power density exceeded 0.88 W/cm^3, and the average power conversion efficiency was up to 18%. This high power generation enabled red, green, and blue light-emitting diodes to turn on after only tens of times bending the generator. This approach offers a breakthrough in realizing a high-performance flexible piezoelectric energy harvester for self-powered electronics.

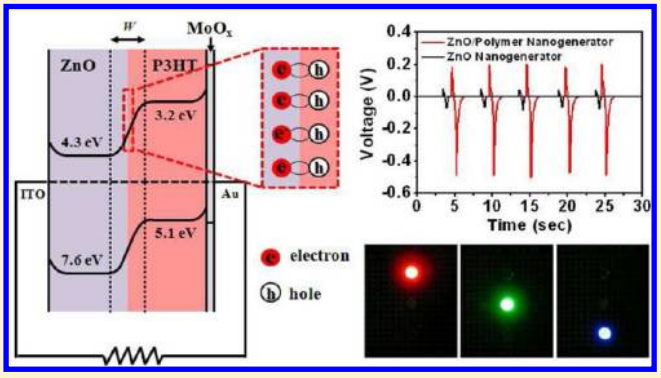

KEYWORDS: *Piezoelectricity, nanogenerator, zinc oxide, polymer, carrier passivation, piezoelectric potential screening effect*

With the recent surge in wireless microelectromechanical systems and nanoelectromechanical system devices, there is increasing demand to harvest energy from the immediate environment, exploiting thermal gradients, solar energy, mechanical vibrations, and biofluids, to create self-powered systems. In particular, mechanical vibrations with irregular amplitudes and frequencies, including human physical motion (such as body movement and muscle stretching), hydraulic energy (such as body fluid and blood flow), air flow, and acoustic/ultrasonic waves, are ubiquitous.[1,2] The piezoelectric energy harvester is a novel device that has been developed to capture this type of energy to power microelectronic devices. Piezoelectric energy harvesters using materials, such as lead zirconate titanate (PZT), polyvinylidene fluoride (PVDF), and barium titanate (BTO), have great potential for sustainable operation of wireless electronic devices.[3−9] However, the high impedance characteristics and high permittivity of such piezoelectric materials lead to low output currents, and this problem must be overcome in creating a power source for self-powered wireless devices. Piezoelectric nanogenerators have recently been demonstrated using materials with piezoelectric and semiconducting coupled properties, such as zinc oxide (ZnO), cadmium sulfide, and gallium nitride, but their output power density is still low for practical application.[1,2,10−20]

The piezoelectric semiconductor material ZnO can generate an intrinsic piezoelectric potential of a few volts as a result of its mechanical deformation, but free carriers exist in ZnO which usually screen some part of the piezoelectric potential that is generated. Consequently, although the output current from ZnO is much larger than that from insulating piezoelectric materials, such as PZT, PVDF, and BTO, the output voltage from ZnO is low as a result of the piezoelectric potential screening effect, resulting in low overall output power generation. The present work seeks a novel approach that dramatically enhances piezoelectric power generation, by introducing a conjugated polymer usually used in organic solar cells and

Received: December 16, 2011
Revised: March 3, 2012

   dx.doi.org/10.1021/nl204440g | *Nano Lett.* XXXX, XXX, XXX−XXX

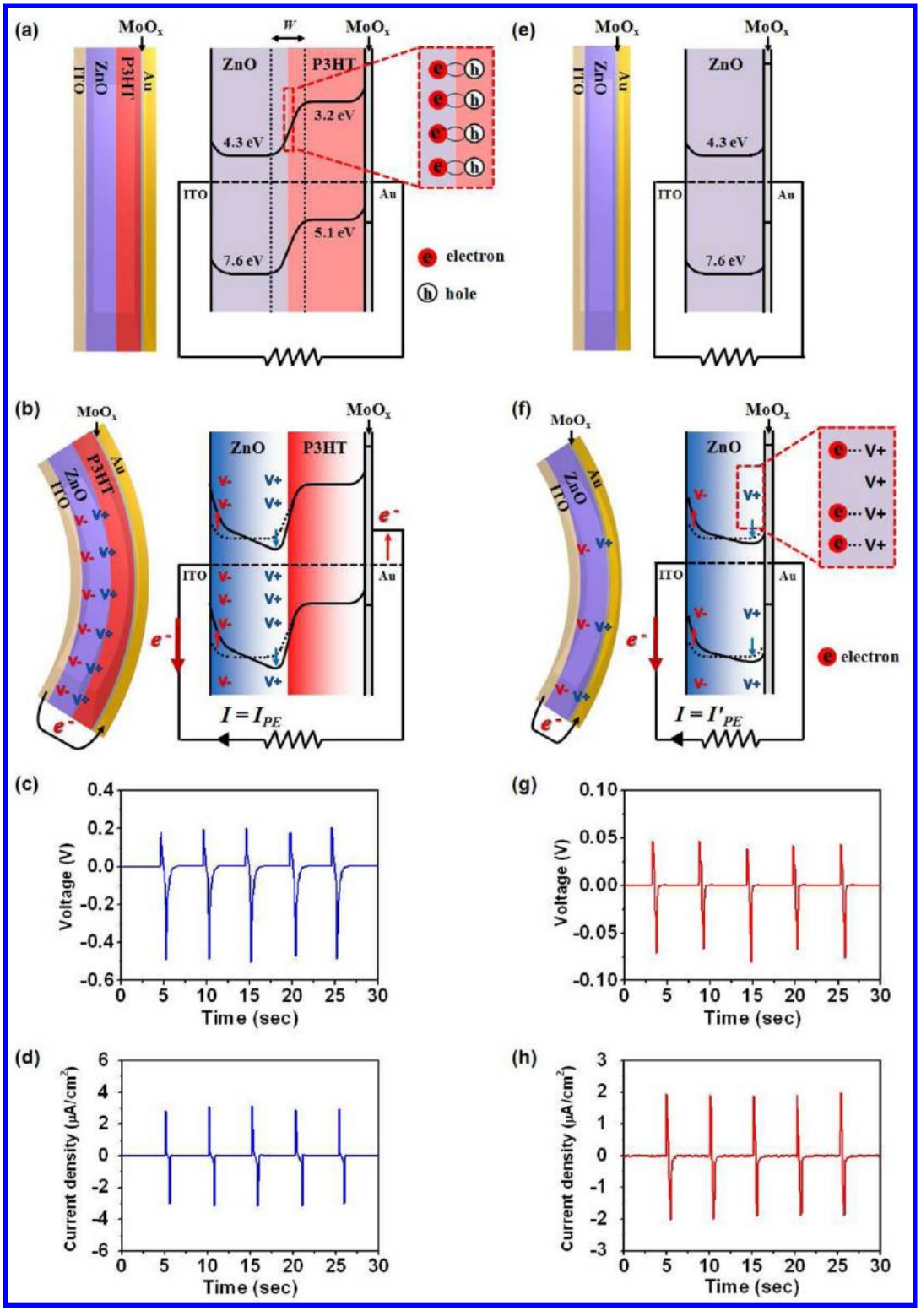

Figure 1. (a) Schematic illustration of ZP-NG with band diagram, at the interface of ZnO−P3HT free electrons in ZnO passivate, attracting holes from P3HT and p−n junction formation. (b) Working principle of ZP-NG undergoing forward bending, such that piezoelectric-induced electrons flow from the ITO electrode to the Au electrode and create new equilibrium states. (c) Measured output voltage from ZP-NG. (d) Measured output current density of ZP-NG. (e) Schematic illustration of Z-NG with band diagram. (f) Working principle of ZP-NG with forward bending, with the piezoelectric potential screened by free carriers in the ZnO layer. (g) Measured output voltage from Z-NG. (h) Measured output current density of Z-NG.

organic light-emitting diodes[21−24] on a piezoelectric semiconductor ZnO layer.

To demonstrate the present approach to power generation in dark condition, we used a p-type poly(3-hexylthiophene) (P3HT) polymer layer on a ZnO thin film. At the ZnO−P3HT interface, holes near the interface from P3HT tend to diffuse into the ZnO layer, and free electrons from the ZnO begin to diffuse into P3HT; the combination of electrons and

dx.doi.org/10.1021/nl204440g | Nano Lett. XXXX, XXX, XXX−XXX

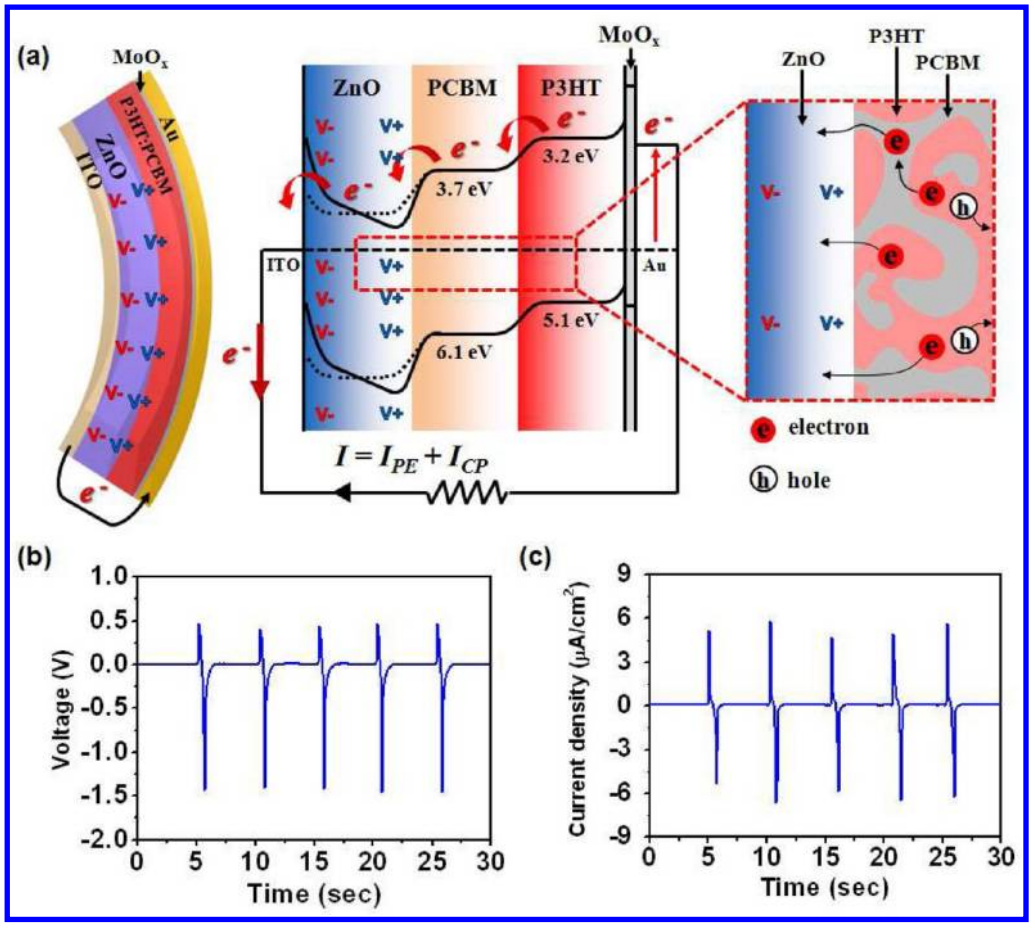

Figure 2. (a) Schematic illustration and working principle of ZB-NG undergoing forward bending. (b) Measured output voltage from ZB-NG. (c) Measured output current density of ZB-NG.

holes forms an interface charge−depletion zone and consequently a p−n junction (Figure 1a). Further as illustrated in Figure 1b, when the ZnO thin film is subjected to a forward bending load,[25,26] a positive piezopotential (V^+) is set up at the ZnO−P3HT interface, and a negative piezopotential (V^-) is at the indium tin oxide (ITO)−ZnO interface surface, which drive the piezoelectric-induced electron flow from the ITO electrode to a gold (Au) electrode through an external load resistor, giving rise to a positive current and voltage pulse. Due to the high Schottky barrier, the electrons accumulate at the interface region between Au and molybdenum oxide (MoO_3); accumulation continues until the potential created by these electrons balances the piezoelectric potential in an equilibrium state. When the strain is released, the piezoelectric potential immediately vanishes, and the electrons accumulated near the Au electrode flow back through the external circuit to the ITO electrode, giving rise to a negative pulse and returning the system to its original state, as shown in Figure 1c,d.

We observed an output voltage of 0.5 V, with a larger current density (3.03 $\mu A/cm^2$), from a power generator fabricated with ZnO−P3HT (referred to below as ZP-NG) than from a power generator fabricated with ZnO layer (called as a Z-NG), which produces an output voltage of just 0.08 V and a current density 1.93 $\mu A/cm^2$, as shown in Figures 1e−h. This enhancement in the output voltage is due to the increase in the piezoelectric potential via neutralization (passivation) of the free electrons existing in the ZnO layer by attracting holes from P3HT and p−n junction formation. When two capacitors are connected in series, their overall capacitance is less than that of either. The ZnO−P3HT system is a combination of two capacitors connected in series during bending: one is the ZnO layer itself during bending, which acts as a capacitor, and the other is the ZnO−P3HT p−n junction. The total capacitance of ZP-NG is therefore less than that of Z-NG. The reduced capacitance of ZP-NG also enhances the observed output voltage. We obtained asymmetric voltage pulses from ZP-NG with a lower enhancement magnitude (0.2 V, a value 2.5 times greater than for Z-NG) of positive voltage pulses and a greater enhancement (0.5 V, a value 6 times higher than for Z-NG) of negative voltage pulses.

The 2.5-fold enhancement in positive voltage pulses is attributed to enhancement of the piezoelectric potential by free carrier passivation. The further enhancement in negative voltage pulses is due to an increased difference in Fermi levels between ITO and Au electrodes, which comes about when more carriers are pumped into the Au electrode due to the strong Schottky barrier on this side of the device. The larger current density from ZP-NG than from Z-NG is due to the higher piezoelectric potential, which more efficiently drives the piezoelectric-induced electron flow from the ITO electrode to the Au electrode through an external load resistor.

To further improve our design, we used phenyl-C_{61}-butyric acid methyl ester (PCBM) in P3HT to improve carrier transportation by forming nanoscale P3HT:PCBM (referred to as 'blend') heterojunctions. The p−n junction diode characteristic was confirmed by current−voltage (I−V) measurements

dx.doi.org/10.1021/nl204440g | Nano Lett. XXXX, XXX, XXX−XXX

(see Figure S1, Supporting Information). When a bending load is applied to a ZnO/blend assembled device (referred to as ZB-NG), the piezopotential drives electrons that flow from the ITO electrode to the Au electrode through an external load resistor, giving rise to a positive current and voltage pulse and a negative pulse while the system returns to its original state, as shown in Figure 2. We observed an enormously enhanced output voltage of 1.45 V, 18 times larger than the value (0.08 V) for Z-NG under the same strain of 0.068% (see Figure S2, Supporting Information, for the strain calculation). This huge enhancement in the output voltage is due to an increased piezoelectric potential via passivation of the free electrons in the ZnO layer by attracting holes from P3HT and p−n junction formation and a further reduction in the capacitance of the device due to ZnO−P3HT junction and P3HT−PCBM junction formation.

When capacitors are connected in series, their overall capacitance is less than that of either. The ZnO/blend system now comprises a combination of three capacitors connected in series during bending: the first is the ZnO layer during bending, which acts as a capacitor, the second one is the ZnO−P3HT p−n junction, and the third is the P3HT−PCBM junction. The total capacitance of ZB-NG is therefore further reduced relative to ZP-NG and Z-NG. The further reduction in capacitance of ZB-NG leads to further enhancement in the observed output voltage, according to the relation which $Q = CV$. The output voltage measured from ZB-NG shows the same trend of asymmetric pulses as observed from ZP-NG, with less enhancement (0.48 V, about 6 times greater than for Z-NG) of positive voltage pulses and greater enhancement (1.45 V, 18 times greater than for Z-NG) of negative voltage pulses. The enhancement in the positive voltage pulses is due to enhanced piezoelectric potential through passivation of free carriers in the ZnO layer and a further reduction in the total capacitance. The dramatic 18-fold enhancement in negative voltage pulses is due to a further increased difference in Fermi levels between ITO and Au electrodes that is a consequence of the large number of carriers pumped into the Au electrode.

This device gives an output current density of 6.05 μA/cm^2 at a strain of 0.068%; that is more than three times the current density as Z-NG (1.93 μA/cm^2). The larger current density is due to the higher piezoelectric potential that drives the piezoelectric-induced electrons to flow more efficiently from the ITO electrode to the Au electrode through an external load resistor and also to an additional effective electron transport from the blend; PCBM acts as a pathway for electron transport into the blend. The potential generated across the ZnO layer is sufficient (for detailed calculation see Figure S3, Supporting Information) to cause band modulation that leads to band bending at the ZnO−P3HT and P3HT−PCBM junctions; consequently, electrons from P3HT:PCBM can reach the ITO electrode by passing through existing barriers in ZB-NG and contribute to the higher current.

To further confirm our mechanism, we fabricated a device that includes a 100 nm thick silicon dioxide (SiO_2) insulating layer between a ZnO thin film and a blend layer, as shown in Figure S5, Supporting Information. In the case of the ZnO/SiO_2/blend assembled device with SiO_2 layer, the output current density ($\sim$ 1 μA/cm^2) and the output voltage (0.05 V) at a strain of 0.068% were both lower than those (1.93 μA/cm^2 and 0.08 V) for Z-NG. The insulating layer prevents neutralization of free carriers in the ZnO and does not allow electrons from blend to reach the ITO electrode. Consequently, no enhancement is measured in output performance. The output current density and output voltage are reduced further due to the high impedance of the device with a SiO_2 layer. We suggest that the interfaces of ZnO with P3HT and PCBM are vital in enhancing the output power of a piezoelectric power generator.

The energy conversion efficiency of ZB-NG has been estimated. The mechanical strain energy stored under a bending load is $W_s = \Sigma 1/2EAL_0\varepsilon^2$, where E is the Young's modulus, A is the cross-sectional area, L_0 is the original length, and ε is the strain for each layer (see Figure S2 and Table S1, Supporting Information).[27] The total electric energy generated from ZB-NG is calculated as $W_e = \int VI\, dt$. We determined the average energy conversion efficiency is up to 18%, about 36 times larger than that of Z-NG (0.5%).

We observed that the performance of ZB-NG behaved differently depending on the bending configuration. When a device undergoes reverse bending,[26,28] the enhanced output voltage is 0.4 V, as shown in Figure 3. This enhancement is less than that observed in forward bending of the same device.

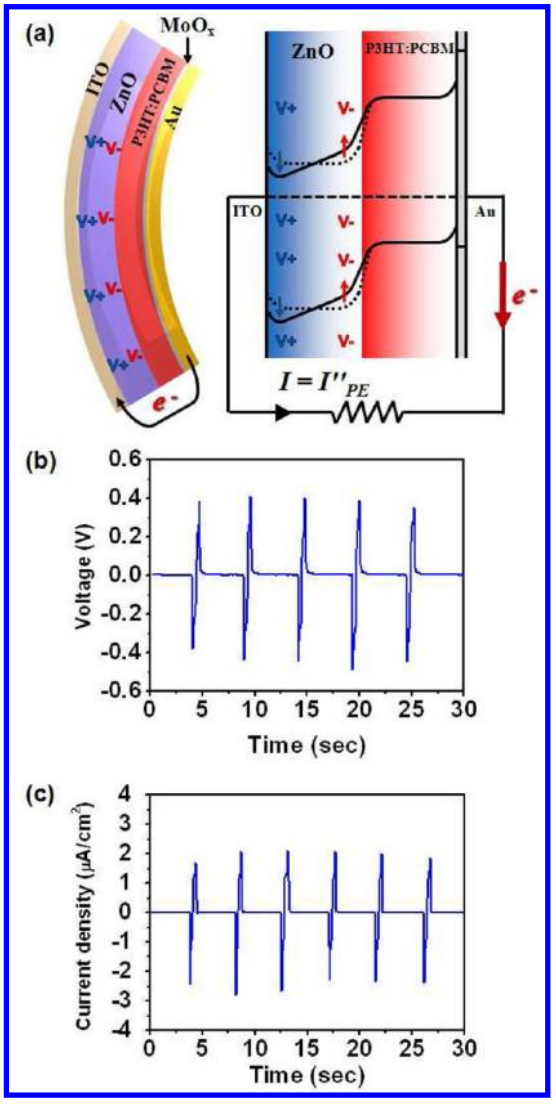

Figure 3. (a) Schematic illustration and working principle of ZB-NG undergoing reverse bending in which piezoelectric-induced electrons flow from the Au electrode to the ITO electrode and create new equilibrium states. (b) Measured output voltage. (c) Measured output current density.

dx.doi.org/10.1021/nl204440g | *Nano Lett.* XXXX, XXX, XXX−XXX

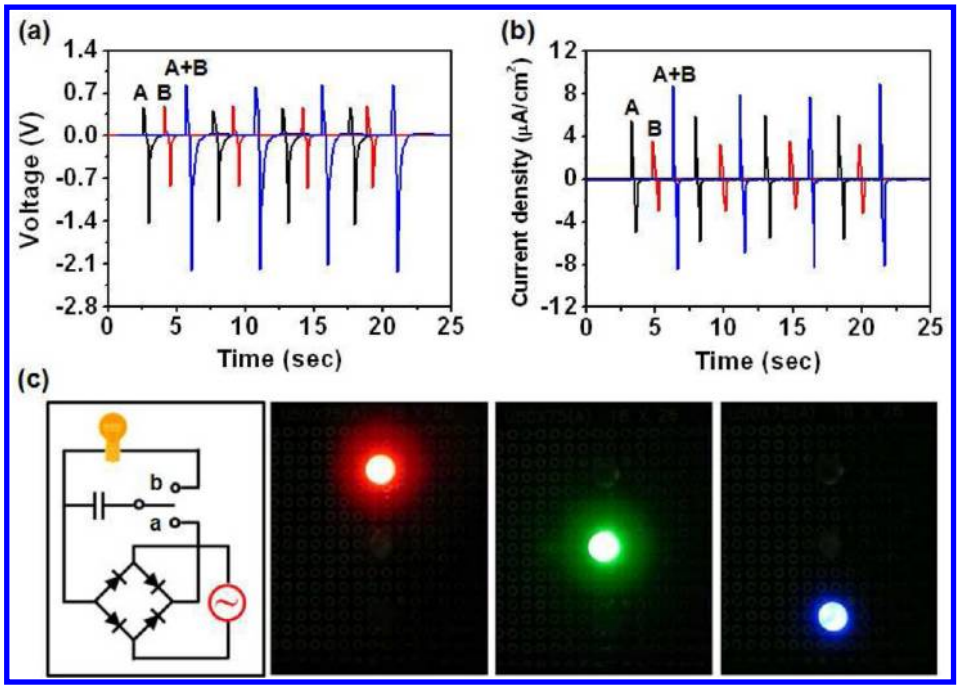

Figure 4. (a) Output voltage with the two devices connected in series. (b) Output current density with the two devices connected in parallel. (c) Application of electrical energy generated by ZB-NG to drive commercial LEDs.

Consequently, in reverse bending, there is no enormous enhancement in the output voltage of symmetric pulses as there is in forward bending. The enhancement is due only to enhancement of the piezoelectric potential by free carrier combination in ZnO and the reduced total capacitance of the device. There is no increased difference in the Fermi levels of the electrodes; a larger number of carriers are not pumped into any electrodes. The Au electrode and the generated negative potential experience a gap of thickness (110 nm). Consequently, a negative piezoelectric potential cannot drive electrons efficiently, in the case of reverse bending, from the Au electrode to the ITO electrode through an external load resistor. As the pressure or force is applied to the device in this direction, a negative piezopotential (V^-) is generated at the interface with the blend and an equal and opposite positive piezopotential (V^+) at the ITO interface. A negative piezopotential cannot therefore attract electrons from the blend, and the strong Schottky contact between MoO_3 and Au does not allow carriers to pass through this side, so that carriers from the blend do not contribute to the output current, and there is no enhancement of the output current.

We have demonstrated high-output performance (1.45 V and 6.05 $\mu A/cm^2$) of ZB-NG using a novel approach involving a huge amplification of power, but for practical application, the output power should be enhanced further. Multiple ZB-NGs can be stacked in a package for enhancing output power. We integrated two ZB-NGs and measured the output current and voltage for each device and integrated device, as shown in Figure 4. A series connection increases the output voltage, and a parallel connection increases the output current density. In series the output voltage was about 2.2 V (Figure 4a), and the output current density in parallel was about 8.13 $\mu A/cm^2$ at a strain of 0.068% (Figure 4b), showing clearly that the output performance is enhanced by integrating ZB-NG. The output current density and voltage were approximately the sum of the output performance of the individual power generators. This result also serves to verify that the measured signal was generated by the piezoelectric power generation rather than the measurement system.[29]

To study a practical application of the ZB-NGs, we designed an integrated charging–discharging circuit,[30] comprised of a power supply (ZB-NGs), a rectifying bridge (1N4148), a switch module, a capacitor (22 $\mu F \pm 10\%$), and commercial LEDs with red, green, and blue emissions, as shown in Figure 4c. When the switch is connected at position "a", the electrical energy attained by the ZB-NGs is stored in a capacitor. Once charging is complete, the switch is moved to position "b" to release the energy and to drive a functional device (in this study, a LED). With a red LED, we only used a single capacitor and a single ZB-NG (device A). After charging by bending the device about 50 times, the red LED lit up for about 1.5 s (see Figure 4c and video, Supporting Information). Green and blue LEDs require greater power, so we used an integrated ZB-NG comprising devices A and B. After about hundred bendings of the integrated ZB-NGs, the green and blue LEDs lit up. This finding demonstrates that ZB-NG can provide a new power source for self-powered systems which can be driven by otherwise wasted mechanical energy.

In summary, we have demonstrated a novel approach for enhancing piezoelectric power generation by introducing the p-type polymer (P3HT) onto the piezoelectric semiconducting thin film (ZnO). Further amplification could be achieved by using a conducting polymer (PCBM). We believe that the amplification is due to enhancement of the piezoelectric potential via free carrier passivation in the ZnO layer, reduction of total capacitance, and increased difference in the Fermi levels of the electrodes. The estimated average energy conversion efficiency was up to 18%, which is about 36 times greater than the conversion efficiency (0.5%) of Z-NG. Using the resulting power generator, it was possible to light up integrated LEDs. This approach provides a promising flexible power supply for realizing self-powered electronics.

dx.doi.org/10.1021/nl204440g | *Nano Lett.* XXXX, XXX, XXX–XXX

■ ASSOCIATED CONTENT

Supporting Information

Experimental details, *I*−*V* characteristic and schematic image of ZB-NG, illustration of device bending to set up the strain, calculated piezoelectric potential in ZnO thin film with strain, schematic with band diagram and output current density of ZB-NG and Z-NG by varying strain, working principle of a nanogenerator with a SiO_2 insulating layer inserted between ZnO and P3HT:PCBM and its measured low output voltage, real image of the electrical circuit for driving commercial LEDs, and a video. This material is available free of charge via the Internet at http://pubs.acs.org.

■ AUTHOR INFORMATION

Corresponding Author

*E-mail: kimsw1@skku.edu (S.-W.K.); dchoi@khu.ac.kr (D.C.); zhong.wang@mse.gatech.edu (Z.L.W.)

Notes

The authors declare no competing financial interest.

■ ACKNOWLEDGMENTS

This work was financially supported by the International Research & Development Program of the National Research Foundation of Korea (NRF) funded by the Ministry of Education, Science and Technology (MEST) (2010-00297), the Energy International Collaboration Research & Development Program of the Korea Institute of Energy Technology Evaluation and Planning (KETEP) funded by the Ministry of Knowledge Economy (MKE) (2011-8520010050), Basic Science Research Program through the NRF funded by the MEST (2010-0015035), a grant (2011-0032151) from the Center for Advanced Soft Electronics under the Global Frontier Research Program of the MEST, and the promotion program for the core faculty of Sungkyunkwan University (2011). D.C. acknowledges financial support by Basic Science Research Program through the NRF funded by the MEST (2011-0008589) and by a grant from the Kyung Hee University in 2011 (KHU-20110489).

■ REFERENCES

(1) Wang, X.; Song, J.; Liu, J.; Wang, Z. L. *Science* **2007**, *316*, 102−105.
(2) Cha, S. N.; Seo, J.-S.; Kim, S. M.; Kim, H. J.; Park, Y. J.; Kim, S.-W. *Adv. Mater.* **2010**, *22*, 4726−4730.
(3) Chen, X.; Xu, S.; Yao, N.; Shi, Y. *Nano Lett.* **2010**, *10*, 2133−2137.
(4) Qi, Y.; Jafferis, N. T.; Lyons, K. Jr.; Lee, C. M.; Ahmad, H.; McAlpine, M. C. *Nano Lett.* **2010**, *10*, 524−528.
(5) Chen, X.; Xu, S. Y.; Yao, N.; Xu, W. H.; Shi, Y. *Appl. Phys. Lett.* **2009**, *94*, 253113.
(6) Chang, C.; Tran, V. H.; Wang, J.; Fuh, Y.-K.; Lin, L. *Nano Lett.* **2010**, *10*, 726−731.
(7) Hansen, B. J.; Liu, Y.; Yang, R.; Wang, Z. L. *ACS Nano* **2010**, *4*, 3647−3652.
(8) Hu, J.; Suryavanshi, A. P.; Yum, K.; Yu, M. F.; Wang, Z. Y. *Nano Lett.* **2007**, *7*, 2966−2969.
(9) Park, K.-I.; Xu, S.; Liu, Y.; Hwang, G.-T.; Kang, S.-J. L.; Wang, Z. L.; Lee, K. J. *Nano Lett.* **2010**, *10*, 4939−4943.
(10) Wang, Z. L.; Song, J. H. *Science* **2006**, *312*, 242−246.
(11) Wang, Z. L. *Adv. Funct. Mater.* **2008**, *18*, 3553−3567.
(12) Corso, A. D.; Posternak, M.; Resta, R.; Baldereschi, A. *Phys. Rev. B* **1994**, *50*, 10715−10721.
(13) Lin, Y. F.; Song, J. H.; Ding, Y.; Lu, S. Y.; Wang, Z. L. *Appl. Phys. Lett.* **2008**, *92*, 022105.
(14) Su, W. S.; Chen, Y. F.; Hsiao, C. L.; Tu, L. W. *Appl. Phys. Lett.* **2007**, *90*, 063110.
(15) Huang, C. T.; Song, J. H.; Lee, W. F.; Ding, Y.; Gao, Z. Y.; Hao, Y.; Chen, L. H.; Wang, Z. L. *J. Am. Chem. Soc.* **2010**, *132*, 4766−4771.
(16) Choi, M.-Y.; Choi, D.; Jin, M.-J.; Kim, I.; Kim, S.-H.; Choi, J.-Y.; Lee, S. Y.; Kim, J. M.; Kim, S.-W. *Adv. Mater.* **2009**, *21*, 2185−2189.
(17) Choi, D.; Choi, M.-Y.; Choi, W. M.; Shin, H.-J.; Park, H.-K.; Seo, J.-S.; Park, J.; Yoon, S.-M.; Chae, S. J.; Lee, Y. H.; Kim, S.-W.; Choi, J.-Y.; Lee, S. Y.; Kim, J. M. *Adv. Mater.* **2010**, *22*, 2187−2192.
(18) Park, H.-K.; Lee, K. Y.; Seo, J.-S.; Jeong, J.-A.; Kim, H.-K.; Choi, D.; Kim, S.-W. *Adv. Funct. Mater.* **2011**, *21*, 1187−1193.
(19) Kumar, B.; Lee, K. Y.; Park, H.-K.; Chae, S. J.; Lee, Y. H.; Kim, S.-W. *ACS Nano* **2011**, *5*, 4197−4204.
(20) Kim, K.-H.; Lee, K. Y.; Seo, J.-S.; Kumar, B.; Kim, S.-W. *Small* **2011**, *7*, 2577−2580.
(21) Aziz, H.; Popovic, Z. D. *Chem. Mater.* **2004**, *16*, 4522−4532.
(22) Aziz, H.; Popovic, Z. D.; Hu, N.-X.; Hor, A.-M.; Xu, G. *Science* **1999**, *283*, 1900−1902.
(23) O'Regan, B.; Gratzel, M. *Nature* **1991**, *353*, 737−740.
(24) Park, S. H.; Roy, A.; Beaupŕe, S.; Cho, S.; Coates, N.; Moon, J. S.; Moses, D.; Leclerc, M.; Lee, K.; Heeger, J. A. *Nat. Photon.* **2009**, *3*, 297−302.
(25) Under the forward bending, dissociated charges are moved in accord into the direction of internal field between electrodes.
(26) Shi, J.; Starr, M. B.; Xiang, H.; Hara, Y.; Anderson, M. A.; Seo, J.-H.; Ma, Z.; Wang, X. *Nano Lett.* **2011**, *11*, 5587−5593.
(27) Morris, A. *A practical guide to reliable finite element modeling*; Wiley: Chichester, U.K., 2007.
(28) Under the reverse bending, dissociated charges are moved in discord into the direction of internal field between electrodes.
(29) Wang, Z. L. *Adv. Mater.* **2008**, *20*, 1−5.
(30) Zhu, G.; Yang, R.; Wang, S.; Wang, Z. L. *Nano Lett.* **2010**, *10*, 3151−3155.